# Interdigitated coplanar electrodes for enhanced sensitivity in a photorefractive polymer

C. W. Christenson,[1],* C. Greenlee,[1] B. Lynn,[1] J. Thomas,[2] P.-A. Blanche,[1] R. Voorakaranam,[1]
P. St. Hilaire,[1] L. J. LaComb, Jr,[1] R. A. Norwood,[1] M. Yamamoto,[3] and N. Peyghambarian[1]

*[1]College of Optical Sciences, The University of Arizona, Tucson, Arizona 85721, USA*

*[2]NanoScience Technology Center, CREOL, College of Optics and Photonics and College of Engineering,
University of Central Florida, Orlando, Florida 32816, USA*

*[3]Nitto Denko Technical, Oceanside, California 92058, USA*

*Corresponding author: cchristenson@optics.arizona.edu*

Organic photorefractive polymer composites can be made to exhibit near 100% diffraction efficiency and fast writing times, though large external slants are needed to project the applied field onto the grating vector. We show here that the use of interdigitated electrodes on a single plane provides similar performance to these standard devices and geometries but without a external slant angle. This new device's structure also greatly improves the diffraction efficiency and sensitivity compared to less slanted standard devices necessary for some real applications, such as holographic displays, optical coherence imaging, and in-plane switching.    © 2011 Optical Society of America

*OCIS codes:*    160.5320, 050.7330, 160.4890.

The photorefractive (PR) effect in organic polymers has found many applications since its discovery in 1991 [1], such as imaging through tissue [2], image correlation for optical security [3], and large-area, multicolor, updatable holographic displays [4,5]. In standard configurations [polymer between two indium tin oxide (ITO) electrodes], the applied field is normal to the polymer plane, but a large field projected in the direction of the grating vector ("projection field") is needed to develop the space-charge field (SCF). This requires slanting the sample between 50° and 70° relative to the writing beams to decrease the angle between the applied field and the grating vector ("projection angle") [6], which is limited in the material due to Snell's Law. Near 100% internal efficiency can be obtained in such geometries [4].

In displays, larger slant angles reduce the resolution and writing intensity inside the polymer, and optimized beam injection systems can be complicated, increasing the space required. Slanting also exacerbates beam walk-off in imaging applications where the temporal coherence length is less than the beam diameter [7]. We present here the use of interdigitated electrodes on a single plane that permit grating recording in PR polymers with a near zero degree projection angle without an external slant angle. These electrodes have been used effectively in other types of systems, such as liquid crystals and piezoelectric transducers [8,9].

The PR composite studied is based on the polymer host matrix poly (acrylic tetraphenyldiaminobiphenyl, PATPD). The chromophore 3-(N,N-di-*n*-butylaniline-4-yl)-1-dicyanomethylidene-2-cyclohexene (DBDC) provides the refractive index change, and $C_{60}$ and N-ethyl carbazole (ECZ) are the photosensitizer and plasticizer, respectively. The weight percent of the PATPD/DBDC/ECZ/$C_{60}$ composite was 49.5/30/20/0.5%. Standard samples were prepared by melt processing the mixture between two uniformly coated ITO glass slides ("biplanar") and 105 $\mu$m spacer beads to set the thickness. Samples on interdigitated electrodes were prepared by melt processing between a single patterned ITO-coated glass

slide and an uncoated top glass layer ("coplanar") at 30 $\mu$m thickness (Fig. 1). The distance between the inner edges of the digits was 100 $\mu$m, and the width of the digits was varied as described below. These electrodes were made in-house by UV lithography of uniform ITO-coated glass substrates using a chrome mask and positive photoresist, followed by etching in $HCl/HNO_3/H_2O$. The absorption coefficient of both devices at 633 nm was 80 $cm^{-1}$.

A major difference between the geometries is the electric field space dependence, which is very uniform over the size of the laser beam for biplanar samples but not for coplanar ones. Calculations of the projection field ($E_X$) from interdigitated electrodes having a width of 25 $\mu$m at 1 kV were performed using the physics simulation program COMSOL (Fig. 2). For biplanar samples slanted at 50°, the projection field is 4.5 V/$\mu$m at all points in the film far from the edges. The coplanar field decreases to this value at a height of 20–30 $\mu$m, indicating that there are few anticipated benefits to making much thicker samples.

The internal efficiency will increase with thickness $d$ up to the over-modulation point for biplanar samples if the field is constant, but the same efficiency can be achieved with less material and a larger index modulation in the Bragg regime. Thus, the relevant parameter is $d\Delta n$. This dependence is not straightforward for
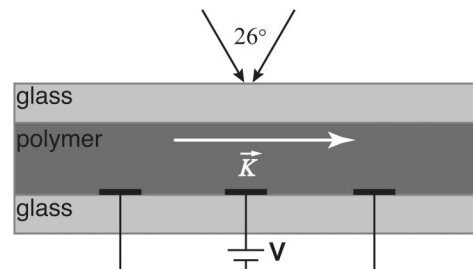


Fig. 1. Schematic of coplanar sample structure (not to scale). Only three electrodes are shown, but 5–10 may be present in the illumination area.
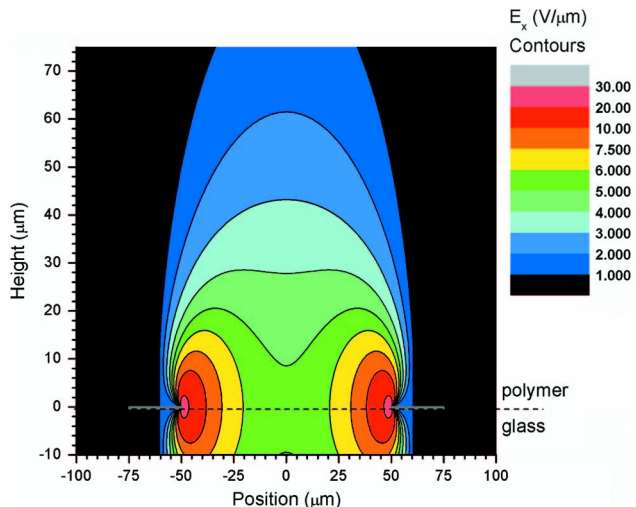
Fig. 2.   Contour map of the field magnitude in the horizontal ($x$) direction above two ITO electrodes (gray bars) with a potential of 1 kV, a separation of 100 $\mu$m and an width of 25 $\mu$m. Only positive valued contours are shown.

coplanar samples, however, so the thickness for biplanar samples is chosen to correspond to that used in the literature. The coplanar sample thickness was then chosen to so that the average projection field would be similar to the 50° slanted biplanar sample (about 4.5 V/$\mu$m). Even though the projection angle is smaller at most points in the coplanar sample, the average projection field is not necessarily larger due to the reduction in the field with height.

As the electrodes widen, the average projection field above the active region increases monotonically (where "active region" refers to the space between electrode digits). However, so does the total amount of null space that occurs directly above the electrode where there the projection field is zero. Thus, there should be an optimum electrode width that balances these two competing effects.

Steady-state degenerate four-wave mixing (DFWM) measurements on coplanar samples were performed at 633 nm with electrode widths of 5, 10, 25, and 50 $\mu$m (Fig. 3). A 1° slant was used to prevent overlap of multi-

ple reflections. The interbeam angle in air was 26° and the total intensity of the $s$-polarized writing beams was 190 mW/cm$^2$ (640 $\mu$m waist). The electrode digits were oriented normal to the plane of incidence. The 10 $\mu$m and 25 $\mu$m wide electrodes have the highest diffraction efficiency; the difference is within sample preparation uncertainty.

DFWM measurements on the biplanar samples (Fig. 4) were carried out in the same manner, but at external slant angles of 10°, 30°, and 50°. The power in each beam was adjusted to provide the same writing intensity at each angle. The diffraction of the standard biplanar samples with smaller slant angles was not significantly above the noise of the system. For biplanar samples the standard theory [6] predicts the diffraction efficiency at a given applied field will generally increase with the slant angle up to the over-modulation point, though the dependence is not simple and few experimental studies of slant effects over a wide range have ever been published [10]. Fundamentally, there is substantial diffraction efficiency in the unslanted geometry with coplanar devices while negligible diffraction is observed in typical devices. In the case of holographic displays [4,5], the slant is around 20°, and the diffraction efficiency of the coplanar sample is at least 3× larger than the biplanar samples at these smaller angles. It is also slightly better than the 50° slanted sample, which could be due to the similar average projection fields in both devices, or because most of the diffraction is occurring in the high field regions near the electrode edge where the projection angle is larger.

The sensitivity was calculated from the transient DFWM, at 4 kV, according to the equation [11]

$$S(t) = \frac{\sqrt{\eta(t)}}{I \cdot t}, \qquad (1)$$

where $\eta$ is the diffraction efficiency, $I$ is the power density of the writing beams, and $t$ is the exposure time. There is an implicit relationship between the index modulation and the efficiency in this equation that assumes the magnitude of the index modulation is uniform. This is true for biplanar samples but not coplanar ones, where information on the average index modulation cannot be
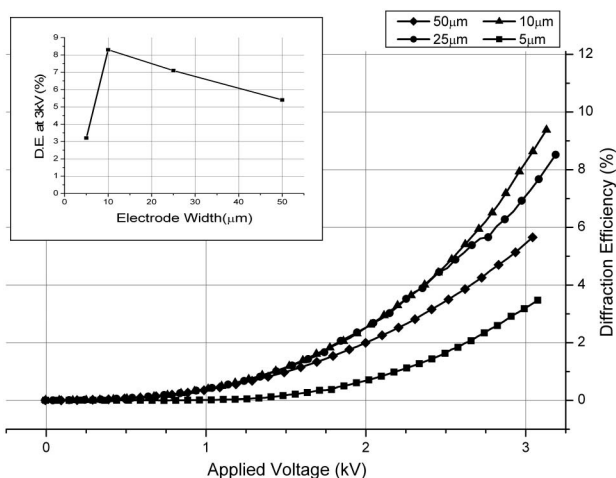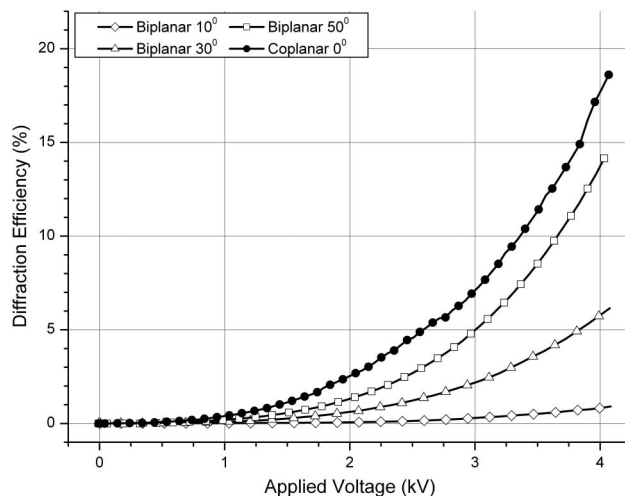


Fig. 3.   Steady-state diffraction of coplanar electrodes with 100 $\mu$m inner spacing and varying width. Inset: Diffraction efficiency at 3 kV trend with electrode width.



Fig. 4.   Steady-state diffraction efficiency, comparing coplanar sample with 25 $\mu$m wide electrodes to biplanar samples with varying external slant angles (shown in key).

**Table 1. Sensitivity Calculated from the Transient Diffraction Efficiency According to Eq. (1) at $t = 0.5$ s and 4 kV**

| Device | Coplanar | Biplanar | Biplanar | Biplanar |
|---|---|---|---|---|
| Slant Angle (°) | 1 | 10 | 30 | 50 |
| $S$(cm$^2$/mJ) | 0.0018 | 0.00038 | 0.0013 | 0.0019 |

obtained solely from the transient data. The sensitivity is not normalized to thickness, since the effect for coplanar samples is still under study, though for biplanar samples the thickness will affect the efficiency as discussed above. Different thicknesses, as well as computer simulations, will be used in future studies to model the diffraction characteristics of nonuniform gratings. (1) is still used to provide a practical comparison of the performance since diffraction efficiency is often the relevant parameter for a given application.

The results are in Table 1 for $t = 0.5$ s, which corresponds to an exposure energy density of $95$ mJ/cm$^2$. The coplanar sensitivity is nearly the same as the 50° biplanar sample, achieving the same diffraction efficiency in 0.5 s, and has 5 times larger sensitivity than the 10° sample.

Two-beam coupling (TBC) measurements were performed in the same respective geometries as for DFWM. With a $640\,\mu$m beam waist, biplanar samples slanted at 50° exhibited about 8% intensity change at $2$ kV, while no energy transfer was observed for coplanar samples. This is due to the alternating field direction for adjacent active regions, shifting the phase of the SCF by 90° and reversing the direction of energy transfer. For this large beam size, several active regions contribute resulting in net zero gain. To measure gain accurately, the beam waist was reduced to $50\,\mu$m and several measurements were performed at discrete positions of the sample in the plane of incidence ($25\,\mu$m steps). Figure 5 shows the results for a sample with $50\,\mu$m wide electrodes at $2$ kV. As expected, the direction of the gain reverses after the sample is moved $150\,\mu$m, corresponding to the spatial period of the interdigitated structure. This verifies not only the PR effect in an unslanted transmission

geometry but also that the field pattern behaves as expected. Note that the diffraction efficiency does not depend on the phase of the SCF, so adjacent regions do not cancel in the DFWM experiment.

In summary, organic polymer devices with interdigitated coplanar electrodes have been shown to exhibit the PR effect in an unslanted transmission geometry. This brings the large projection field benefits of small characterization setups to practical large-area applications, with a 1–5 times increase in the sensitivity. This is expected to be useful for holographic displays, where external slanting increases the system size, and reduces the writing intensity and the resolution, as well as for optical coherence imaging, microscopy, and direct image writing. These developments also enable new applications of PR polymers such as tunable phase masks and in-plane switching. Further studies are underway to elucidate the fundamental physics of these devices.
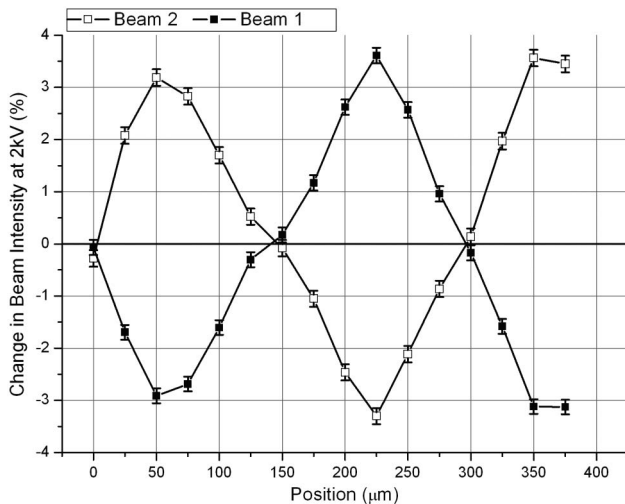
Fig. 5. TBC measurements as the beams were moved relative to the electrodes. Adjacent active regions, where the field direction reverses, are separated by $150\,\mu$m, leading to the periodic signal. There is increased noise due to the lack of lock-in amplifiers.

## References

1. S. Ducharme, J. C. Scott, and W. E. Moerner, Phys. Rev. Lett. **66**, 1846 (1991).
2. M. Salvador, J. Prauzner, S. Köber, K. Meerholz, J. J. Turek, K. Jeong, and D. D. Nolte, Opt. Express **17**, 11834 (2009).
3. B. L. Volodin, B. Kippelen, K. Meerholz, B. A. Javidi, and N. Peyghambarian, Nature **383**, 58 (1996).
4. S. Tay, P.-A. Blanche, R. Voorakaranam, A. V. Tunç, W. Lin, S. Rokutanda, T. Gu, D. Flores, P. Wang, G. Li, P. St. Hilaire, J. Thomas, R. A. Norwood, M. Yamamoto, and N. Peyghambarian, Nature **451**, 694 (2008).
5. P.-A. Blanche, A. Bablumian, R. Voorakaranam, C. Christenson, W. Lin, T. Gu, D. Flores, P. Wang, W. Hsieh, M. Kathaperumal, B. Rachwal, O. Siddiqui, J. Thomas, R. A. Norwood, M. Yamamoto, and N. Peyghambarian, Nature **468**, 80 (2010).
6. W. E. Moerner, S. M. Silence, F. Hache, and G. C. Bjorklund, J. Opt. Soc. Am. B **11**, 320 (1994).
7. M. Salvador, J. Prauzner, S. Köber, and K. Meerholz, Appl. Phys. B **102**, 803 (2010).
8. R. G. Lindquist, J. H. Kulick, G. P. Nordin, J. M. Jarem, S. T. Kowel, M. Friends, and T. M. Leslie, Opt. Lett. **19**, 670 (1994).
9. Y. B. Jeon, R. Sood, J.-h. Jeong, and S.-G. Kim, Sens. Act. A Phys. **122**, 16 (2005).
10. S. P. Bant, D. J. Binks, and D. P. West, Appl. Opt. **41**, 2111 (2002).
11. J. Ashley, M.-P. Bernal, G. W. Burr, H. Coufal, H. Guenther, J. A. Hoffnagle, C. M. Jefferson, B. Marcus, R. M. Macfarlane, R. M. Shelby, and G. T. Sincerbox, IBM J. Res. Dev. **44**, 341 (2000).